Environ. Sci. Technol. **1999**, *33,* 1028−1037

Secondary Organic Aerosol Formation vs Primary Organic Aerosol Emission: In Situ Evidence for the Chemical Coupling between Monoterpene Acidic Photooxidation Products and New Particle Formation over Forests

ILIAS G. KAVOURAS, NIKOLAOS MIHALOPOULOS, AND EURIPIDES G. STEPHANOU*

Environmental Chemical Processes Laboratory (ECPL), Department of Chemistry, University of Crete, 71409 Heraclion, Greece

In a Eucalyptus forest in Portugal were investigated (a) the formation of secondary organic aerosol formed through the condensation of low vapor pressure products of monoterpenes (α- and β-pinene) photooxidation and (b) the chemical structure of these products related to their ability to form new particles. Two isomers of pinonic acid (*cis*- and *trans*-2,2-dimethyl-3-acetylcyclobutylethanoic acid) and norpinonic acid (*cis*- and *trans*-2,2-dimethyl-3-acetylcyclobutylmethanoic acid), pinic acid (*cis*-2,2-dimethyl-3-carboxycyclobutylethanoic acid), pinonaldehyde (2,2-dimethyl-3-acetylcyclobutylethanal), and nopinone (6,6-dimethylbicyclo[3.1.1]heptan-2-one) were detected in all forest aerosol samples. By considering the diurnal concentration pattern of the acidic products and Aitken nuclei observed during the same periods, our results indicated that *cis*- and *trans*-pinonic, *cis*- and *trans*- norpinonic and pinic acids are photooxidation products of α-pinene chemically coupled with new particles formed. Lipids such as *n*-alkanes, *n*-alkanols, *n*-alkanals, and *n*-alkanoic acids determined in the forest aerosol were associated with primary biogenic emissions from Eucalyptus trees.

Introduction

Terrestrial vegetation, such as deciduous and coniferous trees, release substantial amounts of reactive non-methane hydrocarbons (NMHCs), dominantly isoprene and monoterpenes, to the atmosphere (*1, 2*). Recent estimates have shown that biogenic emissions of NMHCs (850 Tg of organic carbon (OC) per year) can easily exceed emissions from man-made sources (125 Tg of OC per year) (*3*). Monoterpenes are highly reactive since their electron-rich double bonds undergo free-radical addition very fast with OH and NO_3 radicals and ozone (*3*−*12*). Although most of the oxidation products of isoprene and monoterpenes remain in the gaseous phase, some of the less volatile organic compounds partition between gas and particulate phase consequently accumulate in the condensed phase and therefore contribute to the particulate mass (*7, 13, 14*).

* Corresponding author phone: +30-81-393628; fax: +30-81-393607/210951; e-mail: stephanou@chemistry.uch.gr.

Aerosol formation in the atmosphere is an important research issue since aerosol may act as cloud condensation nuclei to determine the cloud climate effect (*15, 16*) and could locally be troublesome from a health aspect. Global production rate estimations of secondary organic aerosols show that the forests are the major sources of atmospheric organic particles (*17*). Assuming a range of yields from biogenic hydrocarbons between 5 and 40% (*3, 18*) an estimate of 30−270 Tg POC per year is obtained, comparable to the production of biogenic and anthropogenic sulfate aerosols (90 and 140 Tg per year, respectively) (*17*). On the other hand, higher plants emit particles through electrical generation by leaves (*19*), vegetation decay (*20*), and mechanical abrasion from leaves due to wind velocity (*21*). Unfortunately, very little information is available that would allow a reliable estimation of the contribution of primary biogenic particles to the organic aerosol burden over forested areas (*17*). Furthermore, secondary aerosols contribute to fine particles, while primary particles, from biogenic sources, are larger and thus short-lived compared to secondary aerosols.

The main photooxidation products of isoprene are methacrolein and methylvinyl ketone, methylfuran, methylglyoxal, formaldehyde, and formic acid (*4, 11, 16*). Since their vapor pressure is too high, their ability to form new particles is negligible. However, a synergistic role was observed increasing the formation of particles from α- and β-pinene (*18*). Although the rate constants for the gas-phase reactions of monoterpenes with OH and NO_3 radicals and ozone have been estimated, there are limited available data on their oxidation products in both gaseous and particulate form (*6, 7, 12, 14, 22*). In addition, most of these data originate from experiments performed under simulated conditions in reaction chambers. Indeed, pinonaldehyde, pinonic acid, norpinonaldehyde, norpinonic acid, and pinic acid were determined as the major products of α-pinene oxidation with ozone and OH radicals in chamber studies (3, *5, 6, 10, 23*). Recently, organic nitrates such as the 2-hydroxy-3-nitratepinane and the 3-oxo-2-nitratepinane were proposed to be formed from the α-pinene/NO_3 radicals reaction (*12*). Nopinone is the major compound formed from β-pinene photooxidation (*5, 6, 9, 10*), which is not highly reactive under atmospheric conditions (*9, 10*).

Very recently (*24*) we reported that formation of new particles over a Eucalyptus forest was related to pinonic acid, an acidic photooxidation product of α-pinene. In the present work we report the results of an extensive study concerning the following: (I) The primary organic aerosol emitted by anthropogenic and natural sources by using specific source related tracers (molecular markers). (II) The secondary organic aerosol formed in the atmosphere by the condensation of low vapor pressure photooxidation products of terpenes (α- and β-pinene). (III) The determination of the chemical structure of these products, related to their ability to form new particles in a forest area.

To our knowledge these results demonstrate reliably, for the first time in situ, the chemical structure of carbonyl compounds carboxylic acids, formed via photooxidation of naturally emitted hydrocarbons and predicted by reaction chamber experiments as well as their chemical coupling with secondary aerosol formation. In addition our results allow a chemical differentiation between the formed secondary particles and the biogenic primary emitted ones.

Methodology

Site Characteristics and Sampling. Continuous measurements of meteorological parameters and concentration of

10.1021/es9807035 CCC: $18.00
Published on Web 02/20/1999

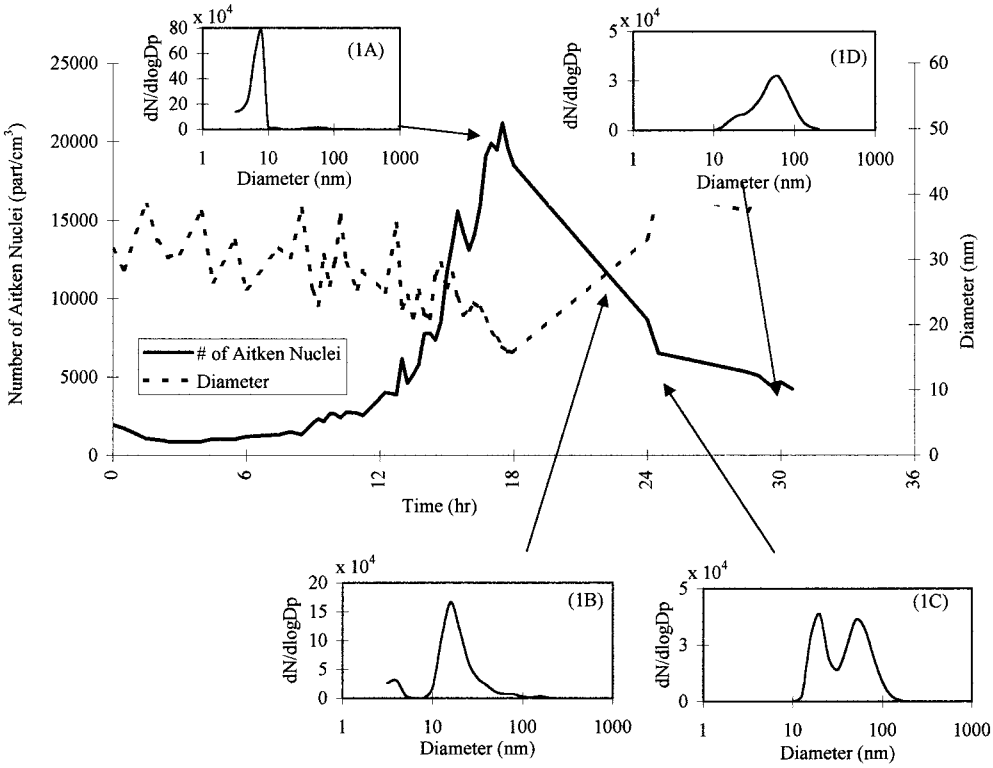

FIGURE 1. Diurnal variation of Aitken nuclei concentration and mean diameter. In the panels are shown the characteristic particle size distributions during the formation (1A) and condensation of new particles after 3 (1B), 6 (1C), and 12 (1D) h during the sampling period II (see Methodology).

O_3, isoprene, monoterpenes, organic acids, and aerosols were performed from August 10 to August 26, 1996, in a *Eucalyptus Globulus* forest located in Tábua (Portugal), situated 100-km inland from the Atlantic coast. Sampling was performed on the top of a 20 m sampling tower, which was situated in the middle of the forest (*25*). An ultrafine Aitken nuclei counter (TSI 3025A), coupled with a diffusion battery (TSI 3040), was used for the determination of Aitken nuclei concentration and size distribution in the 3−200 nm range during the whole experiment period. For the speciation of particle-associated organic compounds, samples were collected on precleaned (550 °C, overnight) 20 × 25 cm glass fiber filters (collection efficiency > 99%) by using a high volume sampler (GMWL-2000, General Metal Works, OH 45002, USA; flow rate 60−75 m^3/h) for the first (I; August 14, to August 16) and second (II; August 18 to August 20) intensive sampling periods of 48 h each. Samples were collected every 6 h during sunlight (8 a.m.−2 p.m. and 2 p.m.−8 p.m.) and every 12 h during nighttime (8 p.m.−8 a.m., next morning). Size distributed aerosol samples were collected at three 12-h intervals (8 a.m.−8 p.m., 8 p.m.−8 a.m., and 8 a.m.−8 p.m.) during the third intensive sampling period (III; August 22 to August 24), by using a five stage (plus backup filter), Sierra Andersen Model 230 Impactor. The impactor was mounted on a high-volume pump. Aerosol particles were separated into six size fractions on glass-fiber filters, according to the following equivalent cutoff diameters at 50% efficiency: first stage > 7.2 μm, second stage 7.2−3.0 μm, third stage 3.0−1.5 μm, fourth stage 1.5−0.96 μm, fifth stage 0.96−0.5 μm, and backup filter < 0.5 μm.

Tests performed have shown that further oxidation of pinonaldehyde, nopinone, pinonic acid, norpinonic acid, and pinic acid on the filter during sampling can be eliminated (*24, 26*).

Fractionation, Derivatization, and Identification of Organic Molecular Markers. A detailed description of the analytical procedure used for extraction, separation, and analysis of the main organic compounds in aerosol and plant leaf wax has been published elsewhere (*27*). Briefly, each sample organic extract (methylene chloride and methanol) was evaporated with a gentle nitrogen stream. The mixture was then dissolved in a small aliquot of *n*-hexane and fractionated by silica gel flash chromatography (*27*). The different compound classes were eluted with the following solvent systems: (1) *n*-hexane for aliphatics; (2) toluene/*n*-hexane for polycyclic aromatic hydrocarbons (PAH); (3) *n*-hexane/methylene chloride for carbonyl compounds; (4) ethyl acetate/*n*-hexane for hydroxyl compounds; and (5) a solution of pure formic acid in methanol for carboxylic acids. Hydroxyl compounds and carboxylic acids were derivatized to their corresponding trimethylsilyl ethers and methyl esters, respectively. The separated organic compounds were analyzed by high-resolution gas chromatography and gas chromatography−mass spectrometry in the electron impact (GC/EI-MS) and chemical ionization with methane as reactant gas (GC/CI-MS). GC/MS-CI analysis of samples was performed on a Finnigan GCQ system by using the same chromatographic conditions as for GC/EI-MS (*27*). The recoveries of molecular markers through the work up procedure presented in this study were previously reported (*27*). The recoveries of monoterpene photooxidation products were 98% for nopinone, 96% for pinonic acid, and 95% for pinic acid.

Materials. Solvents ("SupraSolv" grade) and silica gel (230−400 mesh) were purchased from Merck (Darmstadt, Germany). Standard compounds (pinonic acid, nopinone, and pinic acid) were obtained from Aldrich-Sigma (UK). Whatman (Maidstone, UK) delivered glass fiber filters. All materials were pre-extracted in a Soxhlet apparatus overnight and kept dry until use. Glass fiber filters were baked at 550 °C for 4 h and then kept in a dedicated clean glass container, with silica gel, to avoid humidity and contamination.

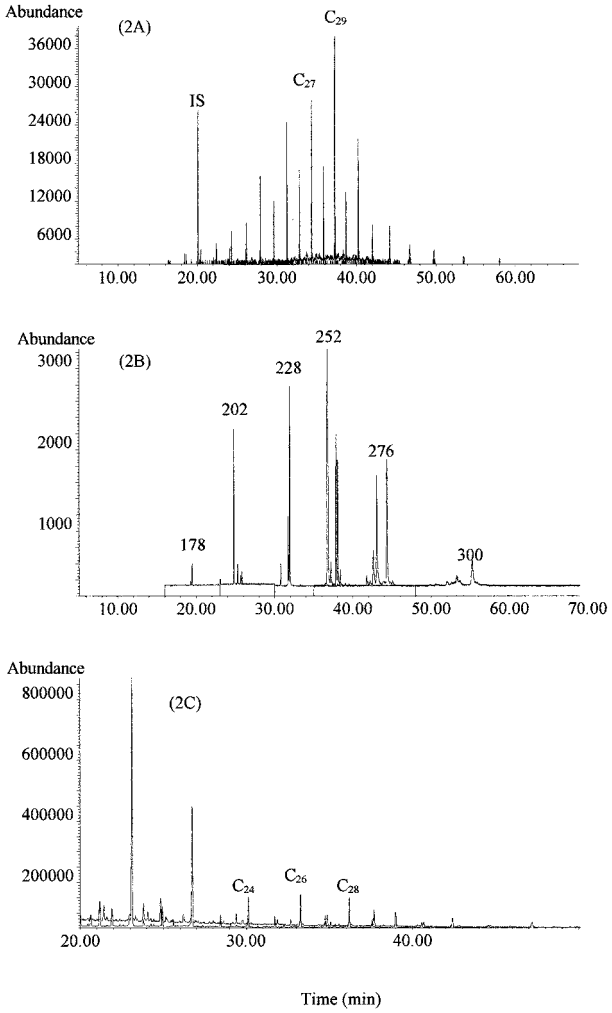

FIGURE 2. Ion chromatogram of the aliphatic (*m/z* 85 + 99, (2A)), aromatic (*m/z* 178 + 202 + 228 + 252 + 276 + 300, (2B)), and of hydroxy (*m/z* 73 + 117, (2C)) fraction isolated from a forest aerosol extract. *Note*: The homologues are noted with their atom carbon number (C_n). The individual PAH compounds are noted with their molecular weight and by increasing retention time: 178; phenanthrene, anthracene; 202, fluoranthene, pyrene; 228, benzo[*a*]anthracene, chrysene/triphenylene; 252, benzo[*b*]-, -[*j*]-, and -[*k*]-fluoranthene; benzo[*e*]pyrene, benzo[*a*]pyrene; 276, indeno[1,2,3-*cd*]pyrene, benzo[*ghi*]fluoranthene; and 300, coronene (*27*).

Results and Discussion

Aitken Nuclei. We recently reported (*24*) that Aitken nuclei concentration, over a Eucalyptus forest, remained constant during the night and increased during daytime by reaching its maximum in the afternoon. In Figure 1, four characteristic particle size distributions demonstrate the formation (Figure 1A) and the condensation of new particles after 3 (Figure 1B), 6 (Figure 1C), and 12 (Figure 1D) h during the sampling period III. This pattern was identical for all sampling periods during the experiment. Indeed, the spectrum during the formation of particles contained only the ultrafine particles mode (nucleation mode; 2−10 nm), which is representative for intensive local production of particles. Three hours later, the maximum moved slightly to the right, indicating that particles were condensed to the Aitken nuclei mode (20−100 nm). The distribution pattern did not change dramatically after 6 h, where a bimodal distribution was observed enriching the accumulation mode (>100 nm). Finally, after 12 h a Gaussian distribution was observed at the accumulation mode due to condensation (probably enhanced by water droplets during the night). Similar observations were reported at a forest site in southern Finland (*28*), providing thus additional evidence for a possible link between forest emissions and new particle formation. In the above study (*28*) data on the chemical composition were not provided.

Air masses back trajectories arriving in the study area were also analyzed (*24*). Despite the observed changes on air masses origin, no changes were observed for the Aitken nuclei concentration and mean diameter's diurnal pattern (*24*). Conversely, we observed that the change of the air mass origin was reflected in the variation of the concentration of nonseasalt sulfate (used as anthropogenic tracer) in the forest aerosol (*24*). These facts indicated that the formation of new particles was due to the local atmospheric chemistry phenomena, rather than to a long-range transport.

Organic Aerosol Compounds Speciation and Quantitation. In Figure 2 are presented ion chromatograms, characteristic of aliphatic hydrocarbons (fragment ions, m/z 85 + 99; Figure 2A), PAH (molecular ions, m/z 178 + 202 + 228 + 252 + 276 + 300; Figure 2B), and methylsilyl ethers of hydroxyl compounds (fragment ions, m/z 73 + 117; Figure 2C) fractions. In Figure 3 are shown the reconstructed ion chromatograms of the fraction containing the carbonyl compounds (Figure 3A) and of the fraction containing the carboxylic ones (Figure 3B). In Table 1 are given the concentrations of the compounds related to the photooxidation of α- and β-pinene.

Higher molecular weight aliphatic hydrocarbons, *n*-alkanals, *n*-alkanols, and *n*-alkanoic acids, were identified in all samples (Figures 2 and 3). These lipids originated mainly from epicuticular wax of Eucalyptus leaves. Indeed, *n*-alkanes concentrations varied from 16.97 to 47.60 ng/m^3, with no specific diurnal profile. *n*-Alkanes homologues ranging from C_{17} to C_{37} or C_{45}, with maximum at C_{29} (Figure 2A), were determined in all aerosol samples. Their relative homologue distribution pattern was very well correlated with this obtained from Eucalyptus leaf epicuticular wax extract (Figure 4A). The presence of higher than C_{31} homologues in aerosol indicated *n*-alkane input from coniferous trees present in the forest area. The input of biogenic sources was also reflected on the carbon preference index (CPI) (*27*) for the whole range of aerosol *n*-alkanes. CPI values for *n*-alkanes ranged from 1.32 to 3.57 pointing out lower or higher biogenic inputs to the aerosol (*29*). Sampling was carried out in the middle of the forest. Nevertheless, the presence of *n*-alkane homologues lower than C_{25} (*29*) and the unresolved complex mixture of branched and cyclic hydrocarbons (UCM; a marker of unburned petrogenic hydrocarbons input from vehicular traffic) (*27*) indicated contribution from anthropogenic emissions to the forest aerosol. The values of the concentration ratio UCM/*n*-alkane (*29*) ranging from 2.17 to 11.43 confirmed this observation. Furthermore, polycyclic aromatic hydrocarbons (PAH) were also detected (Figure 2B). PAHs total concentration (0.05−0.87 ng/m^3) was lower compared to that reported for other nonurban and rural areas (*29*). The concentration ratio of the nine nonalkylated PAH (produced through combustion) to total PAH was higher than 0.50, denoting pyrolytic PAH emission processes (*29*) probably from neighborhood urban areas. *n*-Alkanol homologues from C_{20} to C_{32} with maximum at C_{26} were detected in all examined samples (Figure 2C). The *n*-alkanols concentration varied from 0.06 to 39.72 ng/m^3. No significant differences were observed among the sampling periods. The strong even-to-odd predominance (CPI > 5.98) indicated also that the presence of this lipid class was due to primary emission from Eucalyptus leaf wax. Furthermore, the homologue distribution patterns of aerosol and Eucalyptus leaf wax *n*-alkanols were also correlated (Figure 4B), confirming thus the above hypothesis. The difference in the homologue with the highest concentration, between aerosol (C_{26}) and leaf wax (C_{28}), is probably due to the difference of volatility between C_{26} and

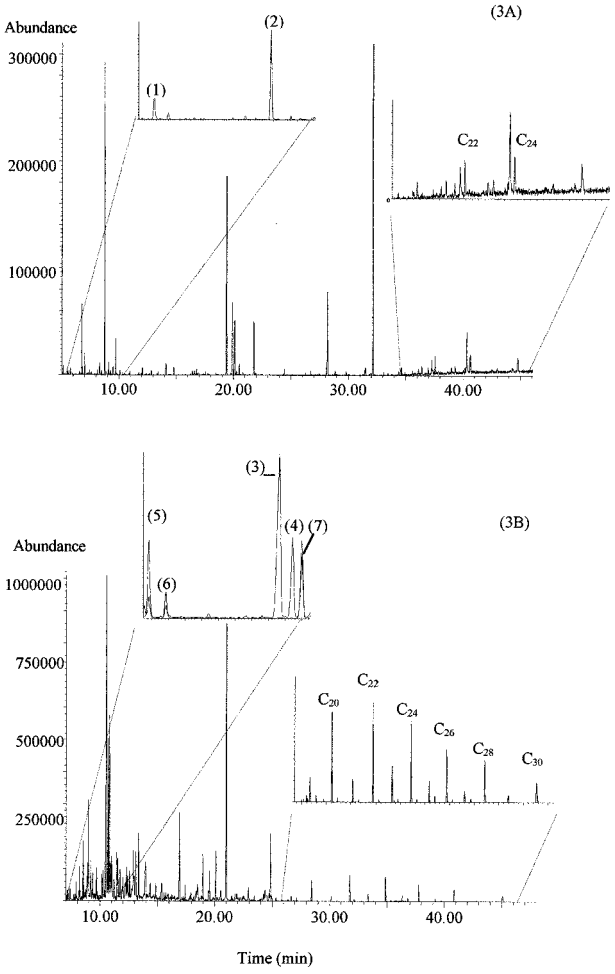

FIGURE 3. Reconstructed ion chromatogram (RIC), with enhanced portions, of the carbonyl (3A) and carboxylic (3B) compound fraction isolated from a forest aerosol extract (see Methodology and ref *27*). *Note*: Compound: 1, nopinone; 2, pinonaldehyde; 3, *cis*-pinonic acid methylester; 4, *trans*-pinonic acid; 5, *cis*-norpinonic acid; 6, *trans*-norpinonic acid; and 7, *cis*-pinic acid methylester; *n*-alkanals (3A) and *n*-alkanoic acid methylesters (3B) are noted with their atom carbon number (C_n).

C_{28} *n*-alkanols. *n*-Alkanals were detected only during the first intensive period (August 14, to August 15). The concentrations varied from 0.33 to 2.24 ng/m^3. The identified *n*-alkanal homologues ranged from C_{22} to C_{26} (Figure 3A) with maximum at C_{22}. The distribution pattern of *n*-alkanals (Figure 4C) was also very similar with that observed for Eucalyptus leaf epicuticular wax suggesting thus their plant origin.

The chromatographic profile of carboxylic acid fraction has shown *n*-alkanoic acid homologues in aerosol samples ranging from C_9 to C_{30} with maximum at C_{16} (Figure 3B). The concentration of *n*-alkanoic acids varied from 13.94 to 232.95 ng/m^3. The homologue distribution was characterized by strong even-to-odd predominance (CPI from 4.64 to 15.64) suggesting a definite biogenic origin for this compound class (*29*). The homologues > C_{20} attest a pronounced higher plant origin (*27, 29*). The comparison of the homologue distribution patterns between aerosol and Eucalyptus leaf wax *n*-alkanoic acids (Figure 4D) indicated the strong primary input of Eucalyptus leaves to the aerosol composition. The low concentration of unsaturated *n*-alkanoic acids in aerosol (0.23−5.95 ng/m^3) could be explained by their rapid photooxidation through the reaction with OH radicals and ozone (*30*). Actually in all analyzed samples, a series of α,ω-dicarboxylic acids was determined. The chain length distribution of this compound class ranged from C_6 to C_{11} and maximized at C_9. The C_9 homologue was the most abundant and is considered to be formed by the photooxidation of unsaturated carboxylic acids such as oleic acid ($C_{18:1}$) (*30*). The highest C_9 α,ω-dicarboxylic acid concentration occurred simultaneously with the lowest concentration of its presupposed precursor (oleic acid).

In addition to the identification of higher molecular weight organic compounds, terpene-skeleton carbonyl and carboxyl compounds were detected in both carbonyl and acidic fractions (see Methodology). The left panel (from 6 to 9 min) of the reconstructed ion chromatogram (RIC) of the carbonyl compounds fraction (Figure 3A) shows two chromatographic peaks corresponding to nopinone (6,6-dimethylbicyclo[3.1.1]-heptan-2-one; compound **1** in Figures 3A and 5) and pinonaldehyde (2,2-dimethyl-3-acetylcyclobutylethanal; compound **2** in Figures 3A and 5). These carbonyl compounds were identified through their mass spectra in electron impact and comparison with the mass spectra of authentic standards (nopinone) and reference mass spectra (pinonaldehyde) (*10*). To further confirm the presence of the above compounds the carbonyl fractions were analyzed by GC/CI-MS. The methane CI spectra of nopinone and pinonaldehyde are presented in Figure 6 (parts A (nopinone) and B (pinonaldehyde)). Both spectra contain the $[M + H]^+$ ions and the expected $[(M + H) - H_2O]^+$ daughter ions characteristic for carbonyl compounds. Nopinone and pinonaldehyde were the most abundant compounds compared to the plant *n*-alkanals (Table 1 and Figure 3A) found also in the carbonyl fraction of the aerosol extract. Pinonaldehyde and nopinone are considered as photooxidation reaction products of α-pinene (*7, 9, 10*) and β-pinene (*3, 9, 10*), respectively. Pinonaldehyde has been reported to be an important product from α-pinene reactions with NO_3 (*12*) and OH radicals and O_3 (Figure 5 and (refs *3, 9, 10, 11, 13*).

As it can be seen in the left panel (7−11 min) of RIC in Figure 3B, the two isomers of pinonic acid (*cis*- and *trans*-2,2-dimethyl-3-acetylcyclobutylethanoic acid; compounds **3** and **4** in Figures 3B and 5), norpinonic acid (*cis*- and *trans*-2,2-dimethyl-3-acetylcyclobutylmethanoic acid; compounds **5** and **6** in Figures 3B and 5), and *cis*-pinic acid (*cis*-2,2-dimethyl-3-carboxycyclobutylethanoic acid; compound (*7*) in Figures 3B and 5) were the acidic products of photooxidation of α-pinene (Figure 5) determined in all aerosol samples collected in this study. These compounds were reported as photooxidation products of α-pinene determined in reaction chamber experiments (*3, 5, 6, 8, 9, 11, 13, 23*). These compounds dominated, in comparison to the plant emitted *n*-alkanoic acids (e.g. $C_{20,}$ C_{22}, C_{24}, C_{26}, C_{28}, and C_{30}; right panel (26−46 min) in Figure 3B), the aerosol organic extract fraction containing the carboxylic compounds (Figure 3B and Table 1). The two isomers of pinonic acid were identified by means of their mass spectra in the electron impact mode and by comparison with the corresponding mass spectra of authentic standards. The GC/CI-MS analysis of the above extracts confirmed further the presence of the two pinonic acid isomers. The CI mass spectrum (Figure 6C) of the *cis*-pinonic acid isomer contains the $[M + H]^+$ ions and the expected $[(M + H) - CH_3OH]^+$ daughter ions. Further fragmentation (*m*/*z* 55, 67, 83) is characteristic for the terpenoid structure. Pinonic acid is one of the main photooxidation reaction products of α-pinene with O_3 in chamber experiments under simulated atmospheric conditions (*3, 6, 10, 23*), while it was only once identified as a component of forest aerosol (*24*). Rearrangements of *cis*- and *trans*-pinonic acid isomers in the presence of solar radiation can be assumed. Interconversion of the pinonic acid isomers in the presence of ultraviolet light is supported by the fact that during daylight the mean concentration ratio, deduced from concentrations in Table 1, of *trans*- to *cis*-pinonic acid was 0.43 ± 0.04 (8−14; Table 1) and 0.47 ± 0.09 (14−20; Table 1). Conversely, during the night this ratio decreased to 0.14 and

TABLE 1. Measured Aerosol Concentrations of α- and β-Pinene Photooxidation Products[a]

	concentration (ng/m³)										
time (h)	pinon-aldehyde	nopinone	*cis*-pinonic acid	*trans*-pinonic acid	*cis*-norpinonic acid	*trans*-norpinonic acid	*cis*-pinic acid	Σcarbonyl	wax *n*-alkanals	Σcarboxylic	wax *n*-alkanoic acids
Sampling Period I											
8−14	8.77	2.36	13.80	5.45	0.27	0.03	*4.85*	11.13	0.33	24.40	14.13
14−20	5.63	1.48	60.09	25.78	12.13	6.60	25.11	7.11	2.24	129.71	21.07
20−32	32.12	13.24	11.13	1.51	4.33	2.34	49.10	45.36	1.47	68.41q	25.23
32−38	4.07	9.01	51.11	24.56	2.21	2.05	82.72	13.10	0.00	162.69	6.17
38−44	0.17	0.29	97.74	42.92	24.29	13.85	63.44	0.46	2.19	242.24	11.08
Sampling Period II											
8−14	0.68	0.09	11.25	4.68	1.19	0.08	*5.14*	0.77	0.00	22.34	1.73
14−20	1.48	0.00	16.94	10.14	0.14	0.00	0.39	1.48	0.00	27.61	0.75
20−32	6.70	0.50	7.05	2.04	1.96	0.35	16.49	7.20	0.00	27.89	12.43
32−38	1.65	0.03	12.16	5.23	0.80	0.38	9.97	1.68	0.00	28.54	16.70
38−44	0.49	0.20	20.70	8.18	2.27	0.07	5.00	0.69	0.00	36.22	10.87

[a] Note: Samples were taken in 6-h intervals during the daytime and 12-h intervals during the nighttime (8−14: 8 a.m.−2 p.m; 14−20: 2 p.m.−8 p.m.; 20−32: 8 p.m.−8 a.m.; 32−38: 8 a.m.−2 p.m.; and 38−44: 2 p.m.−8 p.m.).

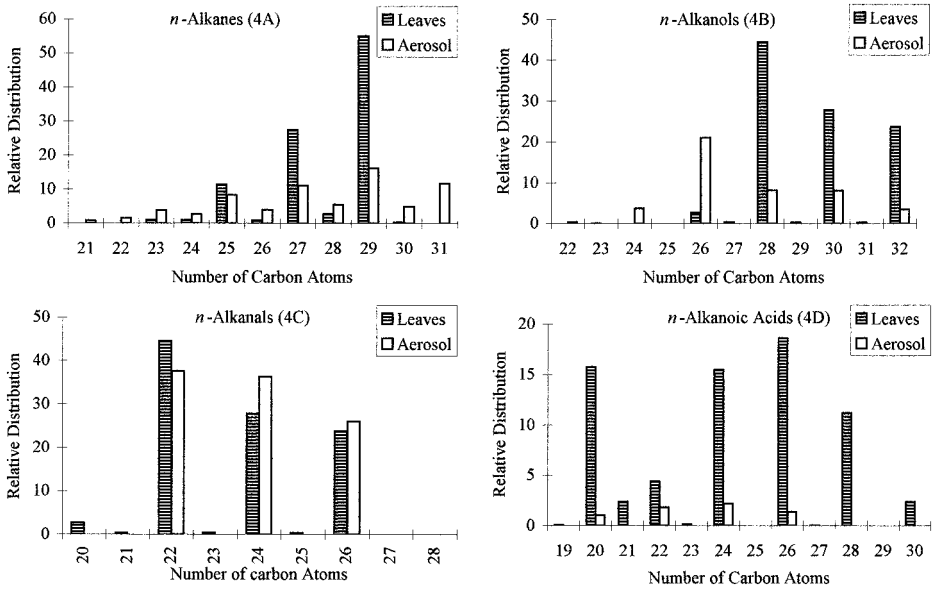

FIGURE 4. Relative distribution of molecular markers in aerosol and Eucalyptus leaf wax. *Note*: The relative distribution for each compound class is shown only for its biogenic components.

0.29, respectively (20−32; Table 1). In addition norpinonic acid was also present, in all aerosol samples collected, as *cis*- and *trans*-isomer (Figure 5). The EI mass spectrum and the corresponding CI spectrum of *cis*-norpinonic acid are shown in Figure 6D,E. The EI spectrum contains the $[M - CH_3]^+$ (m/z 169), $[M - CH_3O]^+$ (m/z 153) ions, while the CI spectrum confirms the molecular ion (m/z 184) through its adducts with the reactant gas, namely $[M + H]^+$ (m/z 185) and $[M + CH_5]^+$ (m/z 201). Norpinonic acid was reported as a reaction product of α-pinene with O_3 in reaction chamber experiments (*6*). Interconversion of the norpinonic acid isomers in the presence of ultraviolet light can also be deduced from the isomers diurnal concentrations (Table 1). The concentration ratio of *trans*- to *cis*-norpinonic acid was generally higher during daytime than during nighttime. Nevertheless its variation was not so definite as for the concentration ratio of the pinonic acid isomers. *cis*-Pinic acid was reported very recently (*23*) for the first time as a secondary organic aerosol component during a reaction-chamber experiment. We identified *cis*-pinic acid, in all aerosol samples, through its EI and CI (methane) spectra and as well as through comparison with authentic standard. The methane CI mass spectrum of *cis*-pinic acid is presented in Figure 6F. The CI spectrum confirms the molecular ion (m/z 214) through its adducts with H (from CH_5^+), namely the $[M + H]^+$ (m/z 215), as well as the daughter ions $[(M + H) - CH_3OH]^+$ (m/z 183) and $[(M + H) - 2CH_3OH]^+$ (m/z 151).

In Table 1 are presented the diurnal concentrations of pinonaldehyde, nopinone, wax *n*-alkanals, *cis*- and *trans*-pinonic acid, *cis*- and *trans*-norpinonic acid, *cis*-pinic acid, and wax *n*-alkanoic acids determined during the two intensive measurement periods. The total concentration of carbonyl (Σcarbonyls; Table 1) and carboxylic (Σcarboxylic; Table 1) compounds, formed through monoterpenes photooxidation, exceeded in the forest aerosol the corresponding concentration of the carbonyl (wax *n*-alkanals; Table 1) and carboxylic compounds (wax *n*-alkanoic acids; Table 1) emitted directly from the forest plants (see also Figure 3A,B).

The analysis of impactor filters was used to evaluate the size distribution of the molecular marker concentration (see diagrams of Figure 7; C, concentration of compound class and dp, diameter of particles) in the aerosol. The size distribution diagram for *n*-alkanes concentration showed a bimodal pattern (Figure 7A). *n*-Alkanes enriching the coarser particles (dp > 3.0 μm) originated most probably from epicuticular wax of Eucalyptus leaves. The second maximum for *n*-alkanes (dp < 2 μm) was similar to the corresponding

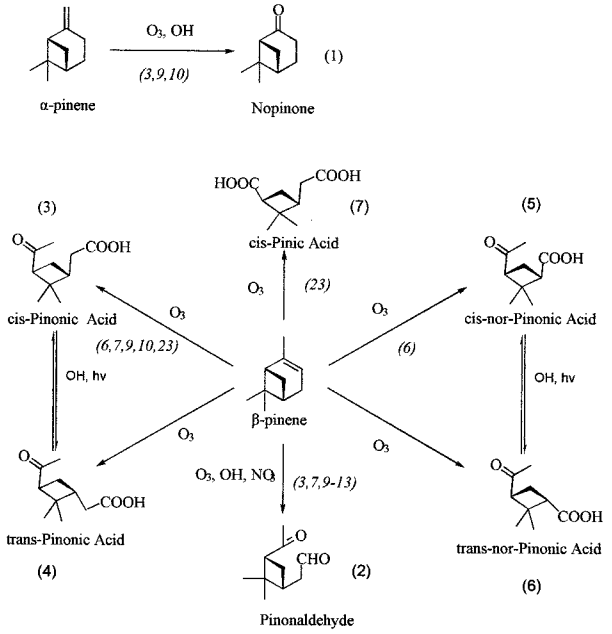

FIGURE 5. Chemical structures of the photooxidation products of α- and *β*-pinene determined in the forest aerosol.

diagram for PAH (Figure 7B), where the maximum (dp < 2 μm) indicated an anthropogenic origin. *n*-Alkanols enriched particles with dp > 7 μm (Figure 7C) denoting also there higher plants origin. Biogenic *n*-alkanoic acids were mostly present in particles having diameter > 1.5 μm (Figure 7D). Conversely, carboxylic photooxidation products of α-pinene (Figure 5) were definitely the acidic species associated with particles having diameter < 500 nm (Figure 7D). Larger particles (> 500 nm) did not contain any detectable quantity of any other photooxidation product of α- and *β*-pinene. According to these observations, directly emitted biogenic organic compounds appear to enrich coarser particles and anthropogenic compounds to be associated with particles having diameter ranging from 0.50 to 1.5 μm. Thus, none of these biogenic organic lipids seems to contribute directly to the formation of Aitken nuclei. Although in most published works (in chamber experiments) pinonic acid was examined as a component of the secondary organic aerosols formed through photooxidation of monoterpenes, the significance of pinonic acid has been observed in chamber experiments very recently (*3*). Our in situ results clearly demonstrate that under real atmospheric conditions the most important compounds contained in the fine (particles with diameter < 500 nm) organic aerosol phase were by far the carboxylic photooxidation products of α-pinene.

Chemical Coupling between Monoterpene Photooxidation Products and New Particles. The diurnal variations of the concentrations and mean diameter of Aitken nuclei are illustrated in Figure 8A,B. Illustrated also are the corresponding diurnal variation of the total concentration of PAH (Figure 8C,D), of particulate cis- and *trans*-pinonic acid (Figure 8E,F), cis- and *trans*-norpinonic acid, and cis-pinic acid (Figure 8G,H), and of particulate pinonaldehyde and nopinone (Figure 8I,J).

The examination of the concentration variation of PAH confirmed that these organic compounds, used as anthropogenic tracer, did not affect the formation of new particles (Figure 8A−D). The diurnal variation of PAH concentration did not follow a clear pattern during the two intensive periods. Moreover this pattern was not correlated with the Aitken nuclei concentration pattern (see Figure 8A−D). Indeed during the first period PAH concentration increased during the day (15−20; Figure 8C) and maximized during the night (20−32; Figure 8C). In the second period a different concentration variation was observed: higher PAH total concentration was measured during the day (8−14 and 32−38; Figure 8D). Similar observations (*24*) were done concerning the correlation of the variation of nonseasalt sulfate (considered as major contributors of aerosol formation). The nonseasalt sulfate concentration pattern was clearly influenced by the origin of air masses but was not correlated with the corresponding Aitken nuclei concentration pattern (*24*).

Recently, we also demonstrated (*24*) that the diurnal variation of the gaseous formic acid and acetic acid was in agreement with the corresponding pattern observed for ozone (60−70 ppbv during daytime and below 10 ppbv at night; (*25*)) and the profile of Aitken nuclei concentration (Figure 8A,B). The gas-phase distributions of the above organic acids suggested that photooxidation of isoprene and monoterpenes emitted from the forest was the source of gaseous formic and acetic acid and new particle formation. Isoprene concentration measured during the same experiment (*25*) showed a similar pattern with that observed for Aitken nuclei and formic acid. In the particulate phase only formate has been detected. The particulate concentration of formic acid accounted for only 8% of the total formic acid (in both gas and particulate phases). This concentration range of formic acid in the particulate phase was in agreement with that reported by Khwaja (*32*). Conversely to the gas phase, the variation of the particulate concentration of formic acid was not correlated with Aitken nuclei concentration. The diurnal variation of particulate *cis*- and *trans*-pinonic acid concentration (Figure 8E,F) followed exactly the same pattern with the corresponding variation of gaseous formic and acetic acid (*24*) and Aitken nuclei concentration (Figure 8A,B). Pinonic acid (both isomers) concentration increased during daytime (8−14, 14−20 and 32−38, 38−44; Figure 8E,F and Table 1), maximizing during the 14−20 and 38−44 sampling periods (Figure 8E,F and Table 1) where new particles were formed (Figure 8A,B). Moreover, their concentration decreased rapidly during the night (20−32; Figure 8E,F and Table 1). Considering that higher ozone concentration (60−70 ppbv, (*25*)) was measured when α-pinene and *β*-pinene concentrations were low (*25*), we could establish that these two acids (associated with particles < 500 nm) are photooxidation products of α-pinene chemically coupled with new particles formed over this forest (*24*).

According to Hatakeyama et al. (*6*) the reaction of α-pinene with ozone gives a singly substituted Criegee intermediate which could rearrange to a vibrationally excited pinonic acid. A part of it is then deactivated to the ground-state pinonic acid (Figure 5, compounds **3** and **4**), while another part decomposes to give C_{n-1} compounds such as norpinonic acid (Figure 5, compounds **5** and **6**). Both isomers of norpinonic acid (*cis*-**5** and *trans*-**6**, Figure 5) followed the same diurnal concentration pattern (Figure 8G) as *cis*- and *trans*-pinonic acid (Figure 8E), in the first intensive period. During the first period the maxima in the concentration of cis- and *trans*-norpinonic acid (Figure 8G) agreed with the maxima of the Aitken nuclei concentration (Figure 8A). In the second intensive period norpinonic acid had a rather different concentration diurnal variation (8−14, 14−20, and 20−32; Table 1 and Figure 8H) than pinonic acid (Table 1 and Figure 8F). Subsequently norpinonic acid presented the same behavior (32−38 and 38−44; Table 1 and Figure 8H) as pinonic acid (Table 1 and Figure 8F).

cis-Pinic acid (compound **7**, Figure 5) was found in comparable concentration to that of pinonic acid (Table 1). The diurnal variation of the concentration of *cis*-pinic acid did not follow a well-defined pattern (Figure 8G,H and Table 1). *cis*-Pinic acid concentration increased during the day and reached its maximum during the night in both intensive periods. This acid was very recently reported as an ozonolysis

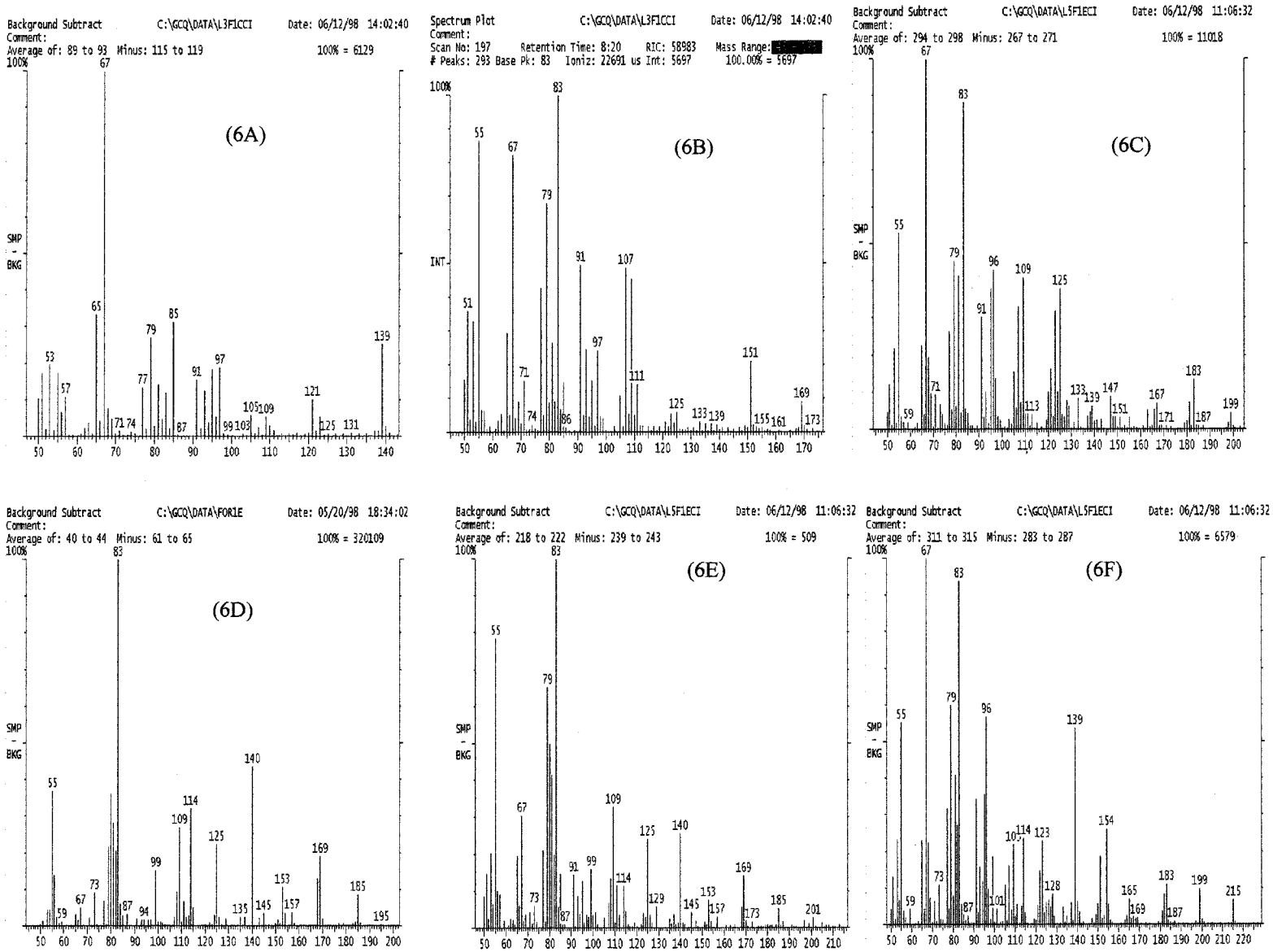

FIGURE 6. Mass spectra of the photooxidation products determined in the forest aerosol. *Note*: Chemical ionization mass spectra of nopinone (6A), pinonaldehyde (6B), *cis*-pinonic acid methylester (6C), *cis*-norpinonic acid methyl ester (6E), and *cis*-pinic acid methyl ester (6F). Electron impact mass spectrum of *cis*-norpinonic acid methyl ester (6D).

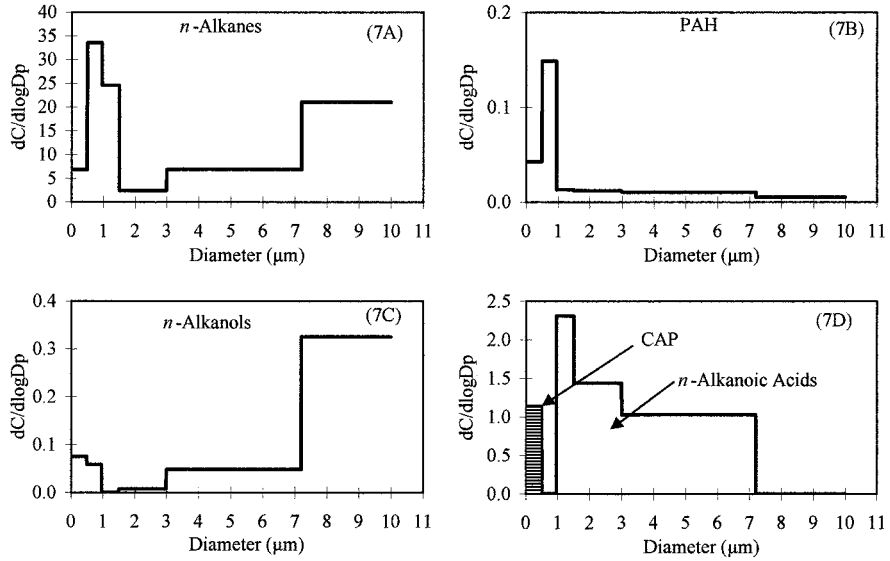

FIGURE 7. Size distribution diagrams of *n*-alkanes (7A), total PAH (7B), *n*-alkanols (7C), biogenic *n*-alkanoic acids (7D), and carboxylic acids formed through the photooxidation of α-pinene (CAP; 7D) concentration determined in forest aerosol. *Note*: C, concentration of compound class and dp, diameter of particles. Twelve-hour samples were collected during the sampling period III (see Methodology).

TABLE 2. Relative Contribution of α- and *β*-Pinene Photooxidation Products in the Total Mass of Condensation Nuclei[a]

	relative contribution (%)								
time (h)	*cis*-pinonic acid	*trans*-pinonic acid	*cis*-pinic acid	*cis*-norpinonic acid	*trans*-norpinonic acid	pinonaldehyde	nopinone	∑carboxylic	∑carbonyl
					Sampling Period I				
8−14	1.04	0.41	0.36	0.02	0.00	0.66	0.18	1.83	0.84
14−20	14.29	6.13	5.97	2.89	1.57	1.34	0.35	30.85	1.69
20−32	1.23	0.17	5.44	0.48	0.26	3.56	1.47	7.58	5.03
32−38	4.91	2.36	7.94	0.21	0.20	0.39	0.87	15.62	1.26
38−44	16.28	7.15	10.56	4.05	2.31	0.03	0.05	40.34	0.08
					Sampling Period II				
8−14	1.47	0.61	0.67	0.16	0.01	0.09	0.01	2.91	0.10
14−20	11.48	6.87	0.26	0.10	0.00	1.01	0.00	18.71	1.01
20−32	8.51	2.46	19.91	2.37	0.42	8.09	0.60	33.67	8.69
32−38	9.03	3.88	7.41	0.60	0.28	1.23	0.02	21.21	1.25
38−44	29.03	11.48	7.02	3.18	0.10	0.69	0.28	50.80	0.97

[a] Note: For sampling time see Table 1.

product of α-pinene (*23*). On the basis of our in situ observations it is difficult to propose a mechanism for the formation of pinic acid. Nevertheless we can assume that the formation of pinic acid and its subsequent participation to the production of new particles is probably a slower process during the day but favored during the night.

The variation of concentration of pinonaldehyde and nopinone (Figure 8I,J and Table 1) presented an interesting diurnal pattern inverse to the respective concentration pattern of Aitken nuclei, formic acid, and cis- and *trans*-pinonic acid. The maximal concentration of pinonaldehyde and nopinone was observed during the night (20−32; Figure 8I,J and Table 1). The reaction between NO_3 and α-pinene has been studied in reaction chamber (*12*) and yielded as main product pinonaldehyde (62 ± 4%). This reaction could be considered a nighttime loss process for α- and *β*-pinene (*12*). On the other hand, the low pinonaldehyde and nopinone concentrations in daytime (8−14, 14−20 and 32−38, 38−44; Figure 8I,J and Table 1) could also be explained by photolysis (3.3 h for pinonaldehyde) and/or reaction with OH radicals (*33*).

These carbonyl compounds have high vapor pressure (5.1 Pa at 298 K for pinonaldehyde (*33*)). Therefore their presence in the particulate matter could be explained by the assumption (*22*) that vapor-phase products condense onto the organic layer of existing particles, even if the gas-phase concentrations of these compounds are below their saturation concentration. The lower temperature occurring during nighttime can support this process. By using adequate sampling techniques the gas-to-particle partitioning of pinonaldehyde and pinonic acid was studied in a conifer forest (*34*). The concentrations of pinonaldehyde and pinic acid in the gas and particulate phases (*34*) were fitted in the model developed by Odum et al. (*22*) to calculate the partitioning coefficient K_{om}. The obtained values for K_{om} were 0.01 to 0.05 for pinonaldehyde and 0.22 to 0.30 for pinonic acid, respectively (*34*). These data (although from another forest) indicate that pinonaldehyde remains preferentially in the gas phase (especially during the daytime), while pinonic acid is associated with the particulate phase.

We assumed, according to Novakov et al. (*15*), that the density of organic particulate matter (particles with dp < 500 nm) is 1 g/cm^3 and that the carbonyl and carboxyl photooxidation products of α- and *β*-pinene are associated with these particles. We could thus calculate the total mass of the Aitken nuclei, from their number and their mean diameter, as well as the relative contribution of these compounds in the formation of fine particles. During the

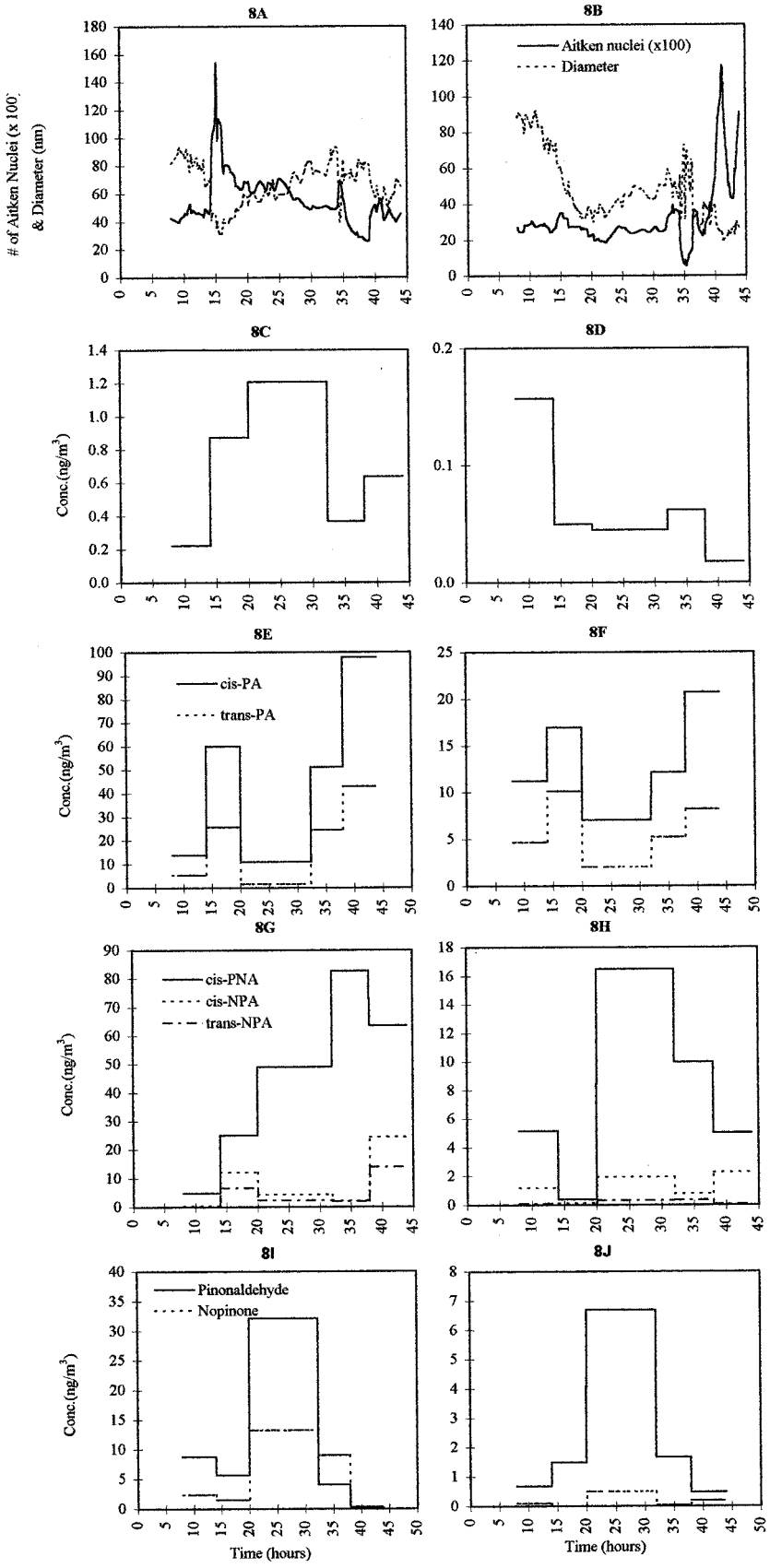

FIGURE 8. Variation of Aitken nuclei mean diameter and concentration (8A,B) during the two intensive measurement periods (I and II; see Methodology). Variation of concentration of the total concentration of PAH (8C,D), cis- (cis-PA) and *trans*-pinonic (trans-PA) acid (8E,F), cis- (cis-NPA), *trans*-norpinonic (trans-NPA), and *cis*-pinic (cis-PNA) acid (8G,H), and pinonaldehyde and nopinone (8I,J). Note: for sampling time see Table 1. Samples were collected during the sampling periods I (8A,C,E,G,I) and II (8B,D,F,H,J) with a high-volume sampler (see Methodology).

daytime, when Aitken nuclei concentration reached its maximum the carboxylic photooxidation products (Σcarboxylic; Table 2) represented the 18.7 to 50.8% of the Aitken nuclei mass. Given the concentrations of the above photooxidation carboxylic compounds (Table 1) and assuming even a low vapor pressure (ca. 10^{-7} Torr as for adipic acid (*35*)), pinonic, norpinonic, and pinic acids were not supersaturated during the events (presuming that we did not have excessive sampling losses). Therefore, on the basis of these results, one could not propose the mode of nucleation of these organic acids occurred in the forest. Nevertheless the results of this study may stimulate discussion about the mechanism of new particle formation under real atmospheric conditions.

Acknowledgments

We thank Maria Apostolaki and Antonios Lemonakis for technical assistance. This research was supported by the Program Environment and Climate (contract CT95-0049) of the European Commission-DGXII.

Literature Cited

(1) Rasmussen, R. A.; Khalil, M. A. K. *J. Geophys. Res.* **1988**, *93*, 1417.
(2) Guenter, A. B.; Monson, R. K.; Fall, R. *J. Geophys. Res.* **1991**, *96*, 10799.
(3) Hofmann, T.; Odum, J. R.; Bowman, F.; Collins, D.; Klockow, D.; Flagan, R. C.; Seinfeld, J. H. *J. Atmos. Chem.* **1997**, *26*, 189.
(4) Gu, C.; Rynard, C. M.; Hendry, D. G.; Mill, T. *Environ. Sci. Technol.* **1985**, *19*, 151.
(5) Arey, J.; Atkinson, R.; Aschmann, S. M. *J. Geophys. Res.* **1990**, *95*, 18539.
(6) Hatakeyama, S.; Izumi, K.; Fukuyama, T.; Akimoto, H. *J. Geophys. Res.* **1989**, *94*, 13013.
(7) Hatakeyama, S.; Izumi, K.; Fukuyama, T.; Akimoto, H.; Washida, N. *J. Geophys. Res.* **1991**, *96*, 947.
(8) Zhang, S. H.; Shaw, M.; Seinfeld, J. H.; Flagan, R. C. *J Geophys. Res.* **1992**, *97*, 20717.
(9) Grosjean, D.; Williams, E. L.; Seinfeld, J. H. *Environ. Sci. Technol.* **1992**, *26*, 1526.
(10) Hakola, H.; Arey, J.; Aschmann, S. M.; Atkinson, R. *J. Atmos. Chem.* **1994**, *18*, 75.
(11) Atkinson, R. *J. Phys. Chem. Ref. Data. Monograph* **1994**, *2*, 1.
(12) Wangberg, I.; Barnes, I.; Becker, K. H. *Environ. Sci. Technol.* **1997**, *31*, 2130.
(13) Yokouchi, Y.; Ambe, Y. *Atmos. Environ.* **1985**, *19*, 1271.
(14) Pandis, S. N.; Paulson, S. E.; Seinfeld, J. H.; Flagan, R. C. *Atmos. Environ.* **1991**, *25A*, 997.
(15) Novakov, T.; Penner, J. E. *Nature* **1993**, *365*, 823.
(16) Fehsenfeld, F.; Calvert, J.; Fall, R.; Goldan, P.; Guenther, A. B.; Hewitt, N.; Lamb, B.; Liu, S.; Trainer, M.; Westberg, H.; Zimmerman, P. *Glob. Biogeochem. Cyc.* **1992**, *6*, 389.
(17) Andreae, M.; Crutzen, P. *Science* **1997**, *276*, 1052.
(18) Pandis, S. N.; Harley, R. A.; Cass, G. R.; Seinfeld, J. H. *Atmos. Environ.* **1992**, *26A*, 2269.
(19) Fish B. R. *Science* **1972**, *175*, 1239.
(20) Schnell, R. C.; Vali, G. *Nature* **1972**, *236*, 163.
(21) Beauford, W.; Barber, J.; Barringer, A. R. *Science* **1977**, *195*, 571.
(22) Odum, J. R.; Hoffman, T.; Bowman, F.; Collins, D.; Flagan, R. C.; Seinfeld, J. H. *Environ. Sci. Technol.* **1996**, *30*, 2580.
(23) Christoffersen, T. S.; Hjorth, J.; Horie, O.; Jensen, N. R.; Kotzias, D.; Molander, L. L.; Neeb, P.; Ruppert, L.; Winterhalter, R.; Virkkula, A.; Wirtz, K.; Larsen, B. R. *Atmospheric Environ.* **1998**, *32*, 1657.
(24) Kavouras, I. G.; Mihalopoulos, N.; Stephanou, E. G. *Nature* **1998**, *395*, 683.
(25) Bonsang, B.; Kanakidou, M.; Stephanou, E. G.; Mihalopoulos, N.; Kavouras, I. G.; Lemonakis, A.; Pio, C.; Nunes, T.; Alves, C.; Seakins, P.; Lewis, A.; Harrison, D., Hunter, M. *Aerosol Formation from Biogenic Carbon;* Report No. 1 to DG XII-Environment and Climate Program on Grant CT95-0049; European Commission: Brussels, 1997.
(26) Geyh, A., Wolfson, J., Koutrakis, P.; Mulic, J. *Development of an active personal O_3 sampler using a hollow tube diffusion denuder*; U.S. Environmental Protection Agency: RTP, NC 27711, 1994; EPA-600A-94/154.
(27) Gogou, A.; Apostolaki, M.; Stephanou, E. G. *J. Chromatog. A* **1998**, *799*, 215.
(28) Makela, J. M.; Aalto, P.; Jokinen, V.; Pohja, T.; Nissinen, A.; Palmroth, S.; Markkanen, T.; Seitsonen, H.; Lihavainen, H.; Kulmala, M. *Geophys. Res. Lett.* **1997**, *24*, 1219.
(29) Gogou, A.; Stratigakis, N.; Kanakidou, M.; Stephanou E. G. *Org. Geochem.* **1996**, *25*, 79.
(30) Stephanou, E. G.; Stratigakis, N. *Environ. Sci. Technol.* **1993**, *27*, 1403.
(31) Hatakeyama, S.; Ohno, M.; Weng, J.; Takagi, H.; Akimoto, H. *Environ. Sci. Technol.* **1987**, *21*, 52.
(32) Khwaja, H. A. *Atmos. Environ.* **1995**, *29*, 127.
(33) Hallquist, M.; Wangberg, I.; Ljungstrom, E. *Environ. Sci. Technol.* **1997**, *31*, 3166.
(34) Kavouras, I. G. Ph.D. Dissertation, University of Crete, 1998.
(35) Tao, Y.; McMurry, P. H. *Environ. Sci. Technol.* **1989**, *23*, 1519.

Received for review July 13, 1998. Revised manuscript received December 30, 1998. Accepted January 11, 1999.

ES9807035